

# 93% pump depletion, 3.5-W continuous-wave, singly resonant optical parametric oscillator

Walter R. Bosenberg, Alexander Drobshoff, and Jason I. Alexander

*Lightwave Electronics Corporation, Mountain View, California 94043*

Lawrence E. Myers\* and Robert L. Byer

*E. L. Ginzton Laboratory, Stanford University, Stanford, California 94305*

Received April 23, 1996

We report two cw, singly resonant optical parametric oscillator (OPO) configurations based on periodically poled lithium niobate that result in significantly higher efficiency and output power than in previous studies. Using four-mirror OPO cavities and pumping with a 1.064- $\mu\text{m}$  Nd:YAG laser, we observe 93% pump depletion and obtain  $\sim 86\%$  of the converted pump photons as useful idler output. The single-beam, in-the-bucket idler output power of 3.55 W at 3.25  $\mu\text{m}$  corresponds to  $\sim 80\%$  of quantum-limited performance. We measure and compare the amplitude noise and spectral bandwidth of the two configurations. We also demonstrate  $>1$  W of tunable cw output over the 3.3–3.9- $\mu\text{m}$  spectral range. © 1996 Optical Society of America

Continuous-wave, singly resonant optical parametric oscillators (SRO's) have long been sought for their high efficiency, high stability, and narrow linewidth output. The earliest theoretical study of SRO's predicted 100% conversion efficiency and single-frequency operation for pumping at  $\sim 2.5$  times the oscillation threshold.<sup>1,2</sup> In this Letter we demonstrate a cw SRO with properties similar to the early predictions. This study builds on our previous demonstration<sup>3</sup> of a cw SRO using the nonlinear material periodically poled lithium niobate (PPLN) and a two-mirror linear cavity. Here we investigate four-mirror ring and linear cavities that increase the conversion efficiency and output at the idler wavelength by a factor of  $\sim 2.5$ . The four-mirror ring cavity SRO operates on a single axial mode of the resonated signal wave despite having a multilongitudinal-mode pump (the idler bandwidth is the same as that of the pump), whereas the linear cavity ran on  $>200$  axial modes. The cw SRO's that we report in this Letter are practical devices that operate with high efficiency (93%), high power ( $>3.5$  W), and low noise (1% rms).

Our pump configuration is similar to that used in the research reported in Ref. 3. The pump laser is a prototype single-transverse-mode, multiple-axial-mode, diode-pumped 1.064- $\mu\text{m}$  Nd:YAG laser that is based on Lightwave Electronics Corporations' commercial DCP technology. The output of the pump laser is nearly diffraction limited ( $M^2 \approx 1.1$ ) and has a linewidth of  $\sim 2.2$  GHz (nine axial modes). The pump beam is passed through a variable attenuator and is mode-matched to the optical parametric oscillator (OPO) cavity with a single 150-mm focal-length lens, resulting in a 64- $\mu\text{m}$  beam waist (radius) inside the crystal; 13.5 W of power is available for pumping the OPO's. No optical isolation is used between the pump laser and the OPO cavity.

We characterized the two OPO cavity configurations as shown in Fig. 1. Both configurations use the same PPLN crystal and cavity mirrors. The

PPLN is 50 mm long with an aperture of 15 mm  $\times$  0.5 mm. The crystal has a grating period of 29.75  $\mu\text{m}$  for first-order quasi-phase matching, resulting in signal and idler wavelengths of 1.57 and 3.25  $\mu\text{m}$  at crystal temperatures of  $\sim 180^\circ\text{C}$ . The two end faces of the crystal have antireflection coatings with power reflectivities of 6%, 0.3%, and 7% for each surface at the pump, signal, and idler wavelengths. The crystal was placed in an oven and operated at temperatures of  $>140^\circ\text{C}$  to avoid the effects of photorefraction.<sup>3,4</sup> Both OPO cavities in Fig. 1 consist of four mirrors. The two curved mirrors have 100-mm radii of curvature

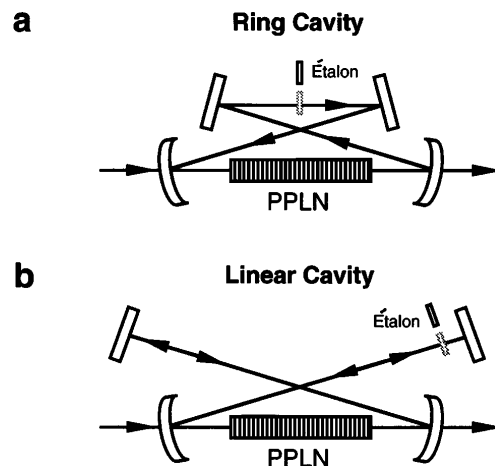


Fig. 1. Schematic of the two OPO cavities that we investigated: a, the four-mirror ring cavity; b, the four-mirror linear cavity. Both cavities use the same crystal and four-cavity optics. The two curved mirrors have 100-mm radii of curvature. The remaining two mirrors are flat. The PPLN crystal is 50 mm long and has a grating period of 29.75  $\mu\text{m}$  for first-order, quasi-phase matching of 1.064- $\mu\text{m}$  pump photons to 1.57- $\mu\text{m}$  signal and 3.25- $\mu\text{m}$  idler photons (crystal temperature is 180  $^\circ\text{C}$ ). Insertion of an intracavity étalon permits quasi-continuous tuning over  $\sim 5$   $\text{cm}^{-1}$ .

and are separated by 154 mm. The input coupler has reflectivities of 2%, 99.7%, and  $\sim 3\%$  at the pump, signal, and idler wavelengths. The output coupler is a coated  $\text{CaF}_2$  substrate with reflectivities of 14%, 99.1%, and  $\sim 11\%$  at the pump, signal, and idler wavelengths. The remaining two mirrors are plano and have reflectivities of 6%, 99.8%, and  $\sim 15\%$  at the pump, signal, and idler wavelengths. The spacing between the curved mirrors and the plano mirrors is 125 mm for the ring cavity and 173 mm for the linear cavity. The two cavities were carefully constructed to have identical resonator mode sizes ( $68 \mu\text{m}$ ) inside the crystal. The round-trip cavity loss for the signal wave was  $\sim 2.2\%$  for the ring cavity and  $\sim 4.0\%$  for the linear cavity. The feedback at the idler wavelength was  $< 0.01\%$  in both configurations, which satisfies the condition for singly resonant operation.<sup>5</sup>

Figure 2 shows the pump depletion and idler output versus pumping for the ring cavity. The threshold of 3.6 W ( $\sim 55 \text{ kW/cm}^2$ ) is slightly higher than the 2.9-W threshold measured for the two-mirror linear cavity under identical pumping conditions ( $\xi = 1$ ; Refs. 3 and 6) because of higher round-trip losses. With 13.5 W of pump radiation, 3.55 W of unresonated  $3.3\text{-}\mu\text{m}$  idler and 1.6 W of the resonated  $1.57\text{-}\mu\text{m}$  radiation were generated. The distinct kink in the input-versus-output power curve at 2.2 times threshold is due to the saturation of the pump depletion. At pump powers less than 2 times threshold the idler quantum slope efficiency<sup>7</sup> is 135%, and at powers greater than 2.5 times threshold the constant pump depletion (93%) reduces slope efficiency to  $\sim 80\%$ . Thus, when pumping the OPO above 2.5 times threshold, we obtain  $\sim 80\%$  of the quantum-limited performance<sup>8</sup> as useful idler output contained in a single, diffraction-limited ( $M^2 \approx 1.1$ ) output beam.

Figure 3 shows the output-versus-input data for the linear cavity. The higher threshold (6 W,  $90 \text{ kW/cm}^2$ ) is due to the additional loss for the resonated wave from the four extra reflections from the coated surfaces during each round trip. Above threshold the pump depletion and idler output data are similar to those of the ring cavity. At  $\sim 2$  times the oscillation threshold the pump depletion saturates to a value of 93%, causing a kink in the idler output curve. The lower part of the curve ( $< 2$  times threshold) has an idler quantum slope efficiency<sup>7</sup> of 150%, which is close to the 135% value for the ring cavity. Overall, other than having different oscillation threshold values, the two cavity configurations have similar conversion performance.

We measured the amplitude stability of the signal radiation for the two OPO cavity configurations with a fast photodiode. For both cavities we observed  $\sim 1\%$  noise (rms) for short time periods (4 s) and 2–5% noise (rms) for longer times periods (30 min) at pump levels of 13.5 W. In a previous study, with a two-mirror linear cavity and a pump focusing parameter,  $\xi > 0.8$ , we observed a sudden onset of amplitude noise in the OPO output when pumping at  $> 1.7$  times threshold.<sup>3</sup> Neither of the four-mirror cavities displayed this noisy behavior, despite having a focusing parameter of  $\xi = 1$  and operating considerably higher than 1.7 times threshold. Our present experimental

arrangement is not optimized for low-noise operation, and straightforward improvements in crystal oven temperature control and vibration isolation should reduce the noise to levels well under 1% (rms).

Although the ring and the linear OPO cavities had similar conversion characteristics, their spectral properties were quite different. We measured the spectral linewidth of the OPO's signal output, using nine coated étalons with free spectral ranges of 0.2–33  $\text{cm}^{-1}$ . The ring-cavity OPO consistently operated on a single axial mode of the OPO resonator (signal linewidth  $< 0.02 \text{ cm}^{-1}$ ). The free-running ring OPO typically stayed on one axial mode for as long as

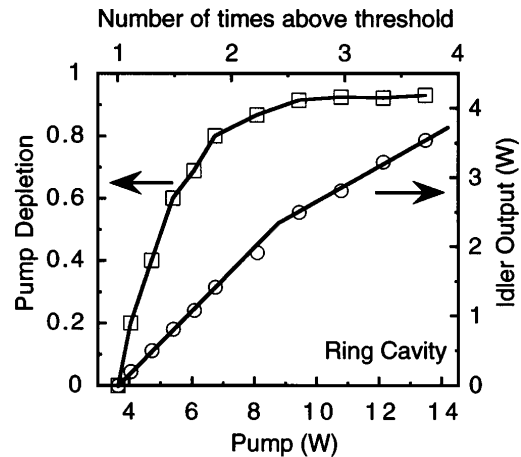


Fig. 2. Pump depletion and idler output versus pump input for the ring cavity operating at an idler wavelength of  $3.25 \mu\text{m}$ . The oscillation threshold is 3.6 W. A maximum of 3.55 W is observed with a 13.5-W pump. The kink in the idler output curve is due to saturation of the pump depletion. At pumping levels higher than 2.4 times threshold, the pump depletion is  $\sim 93\%$ , and the measured idler power is  $\sim 80\%$  of the quantum-limited maximum output.

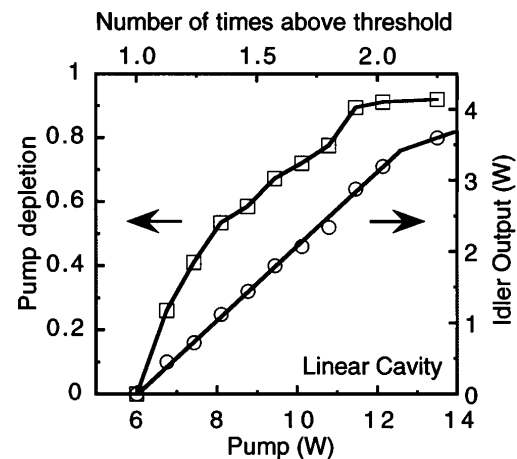


Fig. 3. Pump depletion and idler output versus pump input for the linear cavity operating at an idler wavelength of  $3.25 \mu\text{m}$ . The oscillation threshold is 6.0 W. A maximum power of 3.60 W is observed with a 13.5-W pump. The kink in the idler output curve at 2.2 times threshold is due to saturation of the pump depletion. The idler quantum slope efficiency at pump levels of  $< 2.2$  times threshold is  $\sim 150\%$ .

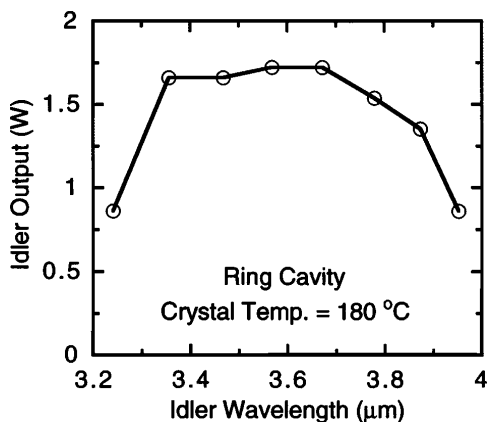


Fig. 4. Idler output versus wavelength for a 25-mm-long multiple quasi-phase matching grating PPLN crystal.<sup>9</sup> Translating the crystal produced idler wavelengths of 3.95–3.24  $\mu\text{m}$  (see text). The tuning range was limited by the losses of the cavity mirror and crystal antireflection coatings. With optimized coatings, multiwatt idler output should be possible over the range of 2.3 to  $>4.2 \mu\text{m}$ .

30 s before it hopped to another axial mode ( $\Delta\nu < \pm 1 \text{ cm}^{-1}$ ). With a 1-mm thick uncoated étalon placed in the cavity as shown in Fig. 1a, the mode hops were constrained to  $\Delta\nu < \pm 0.02 \text{ cm}^{-1}$ . By tilting the étalon, we could tune the device over a range of  $5 \text{ cm}^{-1}$  in a quasi-continuous fashion. Tuning occurred in discrete  $\sim 0.02\text{-cm}^{-1}$  steps (corresponding to the free spectral range of the OPO) as the OPO hopped from axial mode to axial mode. The étalon in the OPO cavity had no effect on the conversion efficiency or output power of the device.

The four-mirror, linear-cavity OPO had spectral properties quite different from those of the ring cavity. Instead of running on a single axial mode of the OPO resonator, the linear cavity tended to run with linewidths of  $\sim 2 \text{ cm}^{-1}$ , corresponding to  $\sim 220$  axial modes. Placing the uncoated 1-mm-thick étalon in the cavity as shown in Fig. 1b reduced the linewidth of the device to  $0.1 \text{ cm}^{-1}$ . Tilting the étalon permitted  $\sim 5 \text{ cm}^{-1}$  of tuning. The intracavity étalon had no effect on the conversion efficiency of the OPO. The spectral behavior of the ring and linear cavities is highly reproducible and is independent of small changes in cavity design. At present the cause for the different spectral behavior of the two cavities is not understood.

We tuned the output wavelengths of the cw OPO by the domain-period tuning technique discussed in previous publications.<sup>3,9</sup> We used a 25-mm-long PPLN crystal having multiple grating structures similar to those reported in Ref. 9. By translating the crystal to allow the pump to pass through regions having domain periods of 28.0–29.75  $\mu\text{m}$ , we produced cw radiation over 3.95–3.25  $\mu\text{m}$  (idler) and 1.45–1.60  $\mu\text{m}$  (signal) in seven discrete steps, as shown in Fig. 4. Intermediate wavelengths can be achieved through varying the temperature of the crystal or fab-

ricating a crystal with finer grating period increments. The extent of the tuning range was limited by the increased cavity losses as the signal wavelength is tuned away from the reflectivity peak of the OPO cavity mirrors.

In summary, we have demonstrated two versatile, mid-infrared cw single-resonant OPO configurations that are approximately 2.5 times more efficient than the device previously demonstrated with a two-mirror linear cavity. The OPO's had a threshold of a few watts, produced  $>3.5 \text{ W}$  of mid-infrared radiation, and demonstrated tuning through the 3–4- $\mu\text{m}$  spectral region. The ring OPO operated on a single longitudinal mode of its resonator when pumped by a multi-longitudinal-mode pump. The linear cavity operated with a linewidth of  $\sim 2 \text{ cm}^{-1}$  (220 modes). Addition of a simple uncoated étalon into both cavities permitted simple, near-continuous tuning with no reduction in output power. These devices validate the high level of performance predicted for cw SRO's by early workers in the field. Future research will be directed at understanding why four-mirror configurations are more efficient than the two-mirror configuration and why the two configurations investigated here have qualitatively different spectral properties.

We acknowledge the assistance of Mark Arbore in fabricating the PPLN crystals used in this experiment. This research was supported by the U.S. Air Force (Eglin Air Force Base and Wright Laboratory, Wright-Patterson Air Force Base) and by the Center for Nonlinear Optical Materials of Stanford University.

\*Present address, U.S. Air Force Wright Laboratory, WL/AAJL, Wright-Patterson Air Force Base, Ohio 45433.

## References

1. L. B. Kreuzer, in *Proceedings of the Joint Conference on Lasers and Optoelectronics* (Institution of Electronic and Radio Engineers, London, 1969), p. 53.
2. S. E. Harris, *Proc. IEEE* **57**, 2096 (1969).
3. W. R. Bosenberg, A. Drobshoff, J. I. Alexander, L. E. Myers, and R. L. Byer, *Opt. Lett.* **21**, 713 (1996).
4. L. E. Myers, R. C. Eckardt, M. M. Fejer, R. L. Byer, W. R. Bosenberg, and J. W. Pierce, *J. Opt. Soc. Am. B* **12**, 2102 (1995).
5. S. T. Yang, R. C. Eckardt, and R. L. Byer, *J. Opt. Soc. Am. B* **10**, 1684 (1993).
6.  $\xi = L/b$ , where  $L$  is the crystal length and  $b$  is the confocal parameter of the Gaussian beam. See S. Guha, F. J. Wu, and J. Falk, *IEEE J. Quantum Electron.* **18**, 907 (1982) for more detail.
7. We define the idler quantum slope efficiency as the slope of the idler-versus-pump-power curve multiplied by the ratio of the idler and the pump wavelengths.
8. Percentage quantum-limited performance,  $(P_i \lambda_i) / (P_p / \lambda_p)$ , where  $P_i$  is the measured idler power,  $P_p$  is the incident pump power, and  $\lambda_p$  and  $\lambda_i$  are the pump and the idler wavelengths. At 100% quantum-limited performance,  $P_i$  would equal 4.4 W for  $P_p = 13.5 \text{ W}$ ,  $\lambda_p = 1.064 \mu\text{m}$ ,  $\lambda_i = 3.25 \mu\text{m}$ .
9. L. E. Myers, R. C. Eckardt, M. M. Fejer, R. L. Byer, and W. R. Bosenberg, *Opt. Lett.* **21**, 594 (1996).